

# Journal of Materials Chemistry C

Accepted Manuscript



This is an *Accepted Manuscript*, which has been through the Royal Society of Chemistry peer review process and has been accepted for publication.

*Accepted Manuscripts* are published online shortly after acceptance, before technical editing, formatting and proof reading. Using this free service, authors can make their results available to the community, in citable form, before we publish the edited article. We will replace this *Accepted Manuscript* with the edited and formatted *Advance Article* as soon as it is available.

You can find more information about *Accepted Manuscripts* in the [Information for Authors](#).

Please note that technical editing may introduce minor changes to the text and/or graphics, which may alter content. The journal's standard [Terms & Conditions](#) and the [Ethical guidelines](#) still apply. In no event shall the Royal Society of Chemistry be held responsible for any errors or omissions in this *Accepted Manuscript* or any consequences arising from the use of any information it contains.

## ARTICLE

# Crack-Free 2D-Inverse Opal Anatase TiO<sub>2</sub> Films on Rigid and Flexible Transparent Conducting Substrates : Low Temperature Large Area Fabrication and Electrochromic Property

Cite this: DOI: 10.1039/x0xx00000x

Received 00th  
Accepted 00th

DOI: 10.1039/x0xx00000x

[www.rsc.org/](http://www.rsc.org/)

Hua Li, Guillaume Vienneau, Martin Jones, Balaji Subramanian, Jacques Robichaud and Yahia Djaoued \*

Two-dimensional (2D) inverse opal (IO) TiO<sub>2</sub>, synthesized by colloidal crystal templating, such as polystyrene (PS) spheres, are particularly interesting because of potential applications in sensors, solar cells, and electrochromic devices. For these applications, high crystallinity is essential for device performance. Usually, to achieve the IO structure with high crystallinity, the PS opal template is first removed by calcination at a temperature of ~ 400 °C, and subsequently to crystallize the amorphous TiO<sub>2</sub>, a temperature higher than 400 °C is needed. This results in cracks and collapse of the macroporous framework. Further, this route is limited to thermally stable substrates, such as glass, which is a significant drawback as the increasing development of technologies and modern electronics requires the design of inexpensive, lightweight, and efficient optoelectronic devices on flexible substrates. In order to circumvent these problems, we developed a 'Dynamic Hard-Template' infiltration strategy for the fabrication of large-area crack-free nanocrystalline (NC) anatase 2D-TiO<sub>2</sub> IO films on rigid transparent conducting substrates and on ITO coated flexible polyethyleneterephthalate (ITO-PET) substrates, by using various sizes of PS spheres. According to this strategy, first a dynamic opal 2D film of PS spheres is self-assembled on the surface of water, followed by the infiltration of preformed anatase TiO<sub>2</sub> nanoparticles sol from the bottom into the PS opal crystal as guest material, thus eliminating the need for high temperature crystallization. The obtained floating PS/TiO<sub>2</sub> opal composite film is deposited on ITO-coated glass and ITO-PET substrates. An optimized low temperature chemical method is adopted to remove the PS template to yield NC anatase 2D-TiO<sub>2</sub> IO films. The films obtained on ITO-PET substrates were successfully used as an active electrode in the fabrication of a flexible electrochromic device.

## Introduction

Two-dimensional (2D) transition metal oxides (TMOs) inverse opal monolayers, based on colloidal crystal templates have received considerable attention in recent years due to their unique properties and potential applications in sensors, solar cells, and electrochromic (EC) devices.<sup>1</sup> For many futuristic applications of these devices, large area crack-free 2D IOs with crystalline TMOs are essential.<sup>2</sup> Among TMOs, nanocrystalline (NC) TiO<sub>2</sub> features several advantages for optoelectronic applications due to its nontoxic character and intrinsic physicochemical properties that combine hardness, semiconducting nature, transparency to visible light, chemical inertia and large specific surface areas.<sup>4-5</sup> Inverse opal nanocrystalline TiO<sub>2</sub> has promising applications where

conventional thin films were applied. Particularly, in the field of electrochromism, (which can be defined as the ability of a material to undergo color change induced by an external electric field,<sup>3</sup>) 2D-TiO<sub>2</sub> IO has not been studied for its optical switching properties. This may be due to the several shortcomings in the conventional synthesis of 2D-TiO<sub>2</sub> IO structures. Conventional fabrication of ordered 2D-TiO<sub>2</sub> IOs monolayers involves three sequential steps: 1. self-assembly of a colloidal crystal template such as polystyrene (PS) on a substrate to form an opal 'static hard template'; 2. infiltration of the TiO<sub>2</sub> precursor within the self-assembled opal template; 3. selective removal of the opal template to yield an inverse opal (IO) structure of the TiO<sub>2</sub>. Unfortunately, attaining a perfect crack-free TiO<sub>2</sub> IO film still remains a challenge, as the cracks mainly arise after the infiltration, and calcination steps. When

the inorganic precursor is converted into the final material, shrinkage is unavoidable since condensation or some decomposition occurs. Moreover, the PS opal template must be removed by calcination at temperature  $\sim 400$  °C.<sup>6</sup> Subsequent increase in temperature is needed to further crystallize the amorphous TiO<sub>2</sub>, and the stress induced interactions between the spheres and the inorganic material results in the collapse of the macroporous framework. Further, such conventional route is limited to thermally stable substrates, such as glass, which is a significant drawback as the increasing development of wireless technologies and modern electronics requires the design of inexpensive, lightweight, and efficient optoelectronic devices such as portable solar cells or EC devices on flexible substrates. In order to circumvent these problems, the direct infiltration of preformed crystalline TiO<sub>2</sub> nanoparticles into the interstitial spaces of the PS opal structure could be a valuable alternative route.

In this context, we present a novel "dynamic-hard-template" infiltration strategy,<sup>7</sup> for the fabrication of large area crack-free morphology-controlled NC anatase 2D-TiO<sub>2</sub> IO films, on conductive transparent ITO coated-polyethyleneterephthalate (ITO/PET) flexible substrate (or ITO coated-glass). Such 2D IO films can be directly used as the working cathode for optoelectronic devices. The strategy is designed to circumvent the issues involved in the preparation of conventional 2D IOs. 1. A dynamic 2D opal film of PS spheres is self-assembled on the surface of water; 2. Since calcination always results in shrink-induced cracks,<sup>8-15</sup> in this work a new strategy is adopted by infiltrating a solution of preformed crystalline anatase TiO<sub>2</sub> nanoparticles from the bottom of the PS opal crystal as guest material; 3. The obtained floating PS/TiO<sub>2</sub> opal composite film is deposited on ITO coated substrates (glass or flexible PET); 4. An optimized low temperature chemical method is adopted to remove the PS template to yield NC anatase 2D-TiO<sub>2</sub> IO films. To the best of our knowledge, this is the first time that large area crack-free fully crystallised NC anatase 2D-TiO<sub>2</sub> IO films deposited on ITO/PET flexible substrate is reported. Also, the optical switching behaviour of EC devices made from the 2D-TiO<sub>2</sub> IO structures was tested.

## Experimental

### Materials

The non-cross linked monodispersed carboxyl polystyrene (PS) spheres aqueous suspensions (PS particles, 5.0 % w/v) were purchased from Spherotech Inc. Before using, they were diluted into 0.5 % w/v with equal volumes of ethanol and water. Prior to use, the ITO coated glass substrates or ITO coated plastic substrates were ultrasonically treated for 15 min, successively in warm water, acetone, ethanol and deionized water. Titanium isopropoxide (Ti(i-PrO)<sub>4</sub>), sodium dodecylsulfate (SDS), Tetrapropylammonium Hydroxide 25 % in water (TPAOH), and ethanol were reagent grade and purchased from Sigma-Aldrich. All the aqueous solutions were prepared with Millipore water (resistance = 18.2 MΩ cm<sup>-1</sup>). The glass substrates were cleaned in a piranha solution (30 % H<sub>2</sub>O<sub>2</sub>:

concentrated H<sub>2</sub>SO<sub>4</sub> = 3:7 v/v) at 100 °C for 15 min, and then washed with Millipore water.

### Synthesis of the sol of preformed crystalline TiO<sub>2</sub> nanoparticles

3.0 ml of Ti(i-PrO)<sub>4</sub> was slowly added to Millipore water. After 1 hour stirring, the crude product was rinsed four times with Millipore water. Wet TiO<sub>2</sub> cake was mixed with 20 ml Millipore water and after addition of 1.2 ml of TPAOH, peptization was carried out for 24 h at 100 °C. The obtained translucent dispersion exhibited a pH of 10 - 11 and it was further diluted with ethanol. The final volume ratio of ethanol to water was 3:7.

### Fabrication of 2D PS opal

To begin with, a clean hydrophilic glass slide was placed on the bottom of a petri dish to avoid the sinking of the colloidal spheres into the water phase. Millipore water was added so as to just submerge the glass slide. Then, the PS spheres suspension (0.5 %w/v) was added drop-wise on the surface of the water, over the glass slide, in order to get a self-assembled monolayer of PS spheres on the water surface. Afterwards, a few drops of 2% SDS solution were added into the water to lower the surface tension, which packed the PS monolayer closely resulting in a 2D PS opal floating over the solution. Once the 2D self-assembly was achieved, the glass slide was gently removed.<sup>7,16</sup>

### Fabrication of 2D-TiO<sub>2</sub> IO structure: "Dynamic Hard-Template" infiltration strategy

Once the PS opal was formed, the sol of preformed crystalline TiO<sub>2</sub> nanoparticles was slowly injected into the water, just under the 2D PS opal monolayer (Step 2, Fig. 1). The volume ratios of different diameter PS suspensions to the sol of preformed crystalline TiO<sub>2</sub> nanoparticles were as follows: 410 nm PS (0.4:8); 530 nm PS (0.45:8); 880 and 920 nm PS (0.5:10). After infiltration, an ITO coated glass substrate (or ITO coated PET flexible substrate) was slid under the PS/TiO<sub>2</sub> opal composite monolayer (Step 3, Fig. 1). Next, the solution was slowly sucked out in order to deposit the film onto the substrate (Step 4, Fig. 1). After drying in air, the 2D PS-TiO<sub>2</sub> opal composite film was dried in an oven at 50 °C overnight, followed by a heat treatment at 100°C. In order to remove the PS spheres and get 2D-TiO<sub>2</sub> IO films, the 2D PS-TiO<sub>2</sub> opal composite films were treated in THF for 4 h.

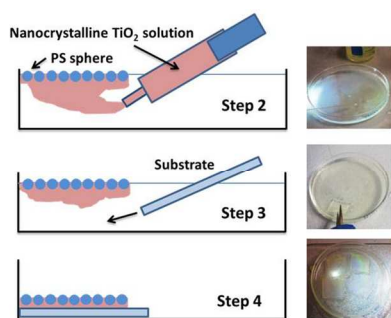


Figure 1 Steps 2 to 4 of the dynamic hard template strategy.

### Fabrication of EC devices from PET flexible substrates

First, an ion conducting layer (ICL) was coated by doctor blade technique on top of the 2D-TiO<sub>2</sub> IO film which had been deposited on an ITO-coated PET flexible substrate according to the strategy described above. Then, another ITO coated PET flexible substrate was gently pressed against the ICL coating to ensure a uniform distribution of the conducting layer. This assembly resulted in an asymmetric EC device with the following configuration: ITO-coated-PET1/TiO<sub>2</sub>IO/ICL/ITO-coated-PET2, as depicted in Fig. 2. The area of the EC devices was  $\sim 2.5 \times 4 \text{ cm}^2$ .

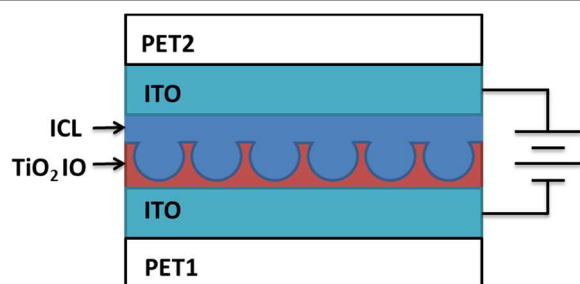


Figure 2 Architecture of the asymmetric EC device constructed from flexible ITO-coated PET substrates.

### Synthesis of the ICL solution

For the synthesis of the ion conducting (IC) solution, first, hybrid ORMOSIL was prepared by an acylation reaction between poly(propylene glycol)bis(2-aminopropyl ether) (2-APPG) with isocyanatopropyltriethoxysilane (ICS) in tetrahydrofuran (THF) in the volume ratio 1:0.1:1. This solution was refluxed for 6 hours at 65°C. After this step, THF was evaporated resulting in a transparent and thick solution. To this hybrid ORMOSIL, an alcoholic solution of LiI (Aldrich powder, 99.9%) + I<sub>2</sub> (BDH, 99.8%, AR) was added to obtain the IC solution. This final solution was viscous with a yellow/brown color.<sup>17</sup>

### Characterization

SEM studies were performed using a S4800 FESEM system from Hitachi. Typically the working distance was 3.2 mm, the accelerating voltage ranged from 1000 to 5000 V, with an emission current of 2300 to 5000 nA.

Micro-Raman spectra were recorded at room temperature with a Jobin-Yvon Labram HR microanalytical spectrometer. The spectra were generated with a 17 mW, 632.8 nm, He-Ne laser excitation and were dispersed with a 1800 gr/mm grating across the 0.8 m length of the spectrograph. The spectral resolution of this apparatus is estimated to be better than 0.5 cm<sup>-1</sup> for a slit width of 150 μm and a confocal hole of 300 μm.

A Biochrom Ultraspec 2000 UV-vis-NIR spectrophotometer was used to record the optical transmittance spectra of the films and of the EC devices in their colored and bleached states.

### Results and discussion

In this work, for the first time a method to prepare crack-free large area NC 2D-TiO<sub>2</sub> IO films by adapting a novel “dynamic-hard-template” infiltration strategy is reported. This method offers the possibility of formation of NC 2D-TiO<sub>2</sub> IO structures on any desired substrates including ITO coated substrates (glass or flexible PET).

#### Mechanism of formation of crack-free 2D PS/TiO<sub>2</sub> opal composite, and 2D-TiO<sub>2</sub> IOs films on ITO glass substrates

To begin with, the “dynamic-hard-template” infiltration strategy was applied for the fabrication of 2D PS/TiO<sub>2</sub> opal composite films on ITO/glass substrates. Opal templates with PS spheres sized from 410 to 920 nm in diameter were formed on the surface of water.<sup>7</sup> The formation of the opal template is governed by two factors (i) the spreading agent role of ethanol and (ii) the hydrophilic nature of the glass surface, which also acts as a buffer storage for the colloidal suspension and controls the speed of PS-spheres self-assembly.<sup>7,16</sup> After the formation of the opal template, an aqueous ethanol sol of preformed crystalline TiO<sub>2</sub> nanoparticles was injected underneath the PS opal crystal. Due to the proper interphase compatibility between the PS spheres and the sol of preformed crystalline TiO<sub>2</sub> nanoparticles, and especially due to capillary action, TiO<sub>2</sub> nanoparticles infiltrated the interstitial spaces in the PS opal film. The PS spheres are held together by the interaction of attractive capillary forces and repulsive electrostatic forces to form the self-assembled opal structure. When the injected TiO<sub>2</sub> nanoparticle sol encounters the PS opal layer, the dominant capillary force between the spheres attract the TiO<sub>2</sub> nanoparticle sol into their interstitial space, which is facilitated by the spreading action of ethanol. During this process, the interstitial space between the PS spheres is slightly enlarged, but the relative position of the spheres is hardly changed due to the still dominant capillary action between the PS spheres, and hence, the opal structure is retained. As the PS spheres are in the liquid air interface, they have the freedom to accommodate guest materials in their interstitial spaces. This infiltration strategy is different from that of an opal already deposited on a substrate, forming a ‘static hard template’, rendering difficult any movement to adjust their position to accommodate guest materials. A waiting time of 20 min was taken to get the sol of preformed crystalline TiO<sub>2</sub> nanoparticles homogeneously infiltrated within the interstitial spaces of the floating PS

spheres monolayer. Then, an ITO coated-glass substrate was inserted into the solution, underneath the floating PS/TiO<sub>2</sub> opal composite film. The liquid in the system was sucked out, and the PS/TiO<sub>2</sub> opal composite deposited onto the substrate. After the formation of the PS/TiO<sub>2</sub> opal composite, it was dried at 50 °C overnight, followed by a heat treatment at 100 °C for 30 minutes, which served to promote the adhesion of the opal composite monolayer to the substrate. Following the optimised 2 steps heat treatment, the PS template could be removed efficiently by THF. Figure 3(a) shows the 2D-TiO<sub>2</sub> IO obtained after the 2 steps heat treatment followed by the removal of the PS spheres by THF. However, when the TiO<sub>2</sub> PS/TiO<sub>2</sub> opal composite films were treated with THF right after the sample had dried at 50 °C overnight, the film moved along the surface of the substrate and the IO structure was destroyed (Fig. 3b). Following the optimised 2 steps heat treatment, the PS template could be removed efficiently by THF.

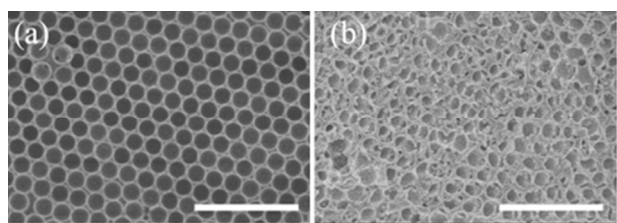


**Figure 3** A side-by-side comparison for 2D-TiO<sub>2</sub> IO films templated by 410 nm PS spheres: a) the film was dried at 50°C overnight followed by a heat treatment at 100°C for 30 minutes, then treated with THF; b) the sample was dried at 50°C overnight, then treated with THF. Scale bars: 2 μm.

### Microstructural, spectroscopic, and optical properties of 2D-TiO<sub>2</sub> IOs films

Fig. 4 (a)-(d) shows SEM images of 2D-TiO<sub>2</sub> IO films on ITO/glass substrates fabricated from different sizes PS spheres of 410, 530, 880, and 920 nm in diameter, respectively, revealing large area crack-free IO films.

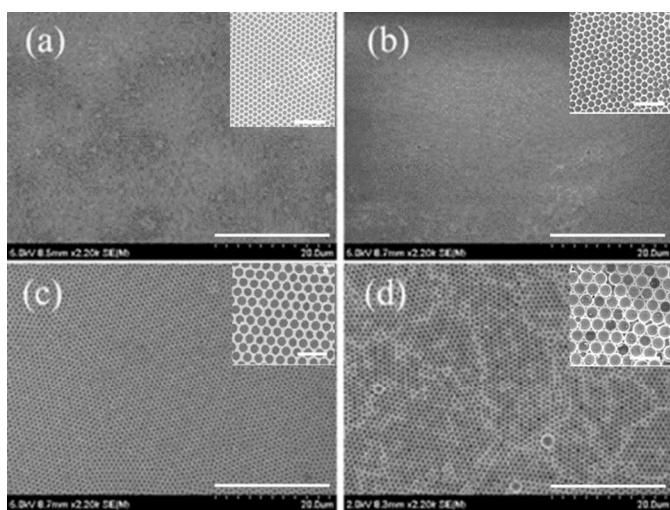


**Figure 4** SEM images of 2D-TiO<sub>2</sub> IO films templated by PS spheres of 410 nm (a); 530 nm (b); 880 nm (c); 920 nm (d), showing crack-free samples. Scale: 20 μm. The insets show magnified SEM images of the corresponding 2D-TiO<sub>2</sub> IO films, displaying the hexagonal symmetry. Scale: 2 μm

The insets in Fig. 4 show magnified SEM images of the corresponding 2D-TiO<sub>2</sub> IO films, displaying the formation of honeycomb structures with hexagonal symmetry. Evidence of minor disorder in the honeycomb structure, similar to crystal defects, is attributed to inevitable sporadic presence of PS spheres of different diameters.

Figure 5(a) shows the corresponding Raman spectra of the 2D-TiO<sub>2</sub> IO films. In all the spectra the characteristic anatase Raman modes of the samples emerge at 148.9 (E<sub>g</sub>), 400.2 (B<sub>1g</sub>), 518.5 (B<sub>1g</sub>) and 640.5 (E<sub>g</sub>) cm<sup>-1</sup>. Also, the broad (19.2 cm<sup>-1</sup>) and high-frequency shift (148.9 cm<sup>-1</sup>) for the main anatase Raman band with respect to the value of commercial anatase TiO<sub>2</sub> powder (142.5 cm<sup>-1</sup>), indicate that the TiO<sub>2</sub> is constituted of fully crystallized TiO<sub>2</sub> nanoparticles. A phonon confinement model has been applied to establish a relation between the crystallite sizes and the main Raman peak position of TiO<sub>2</sub>, and the observed shift corresponds to a crystallite size of ~ 6 nm.

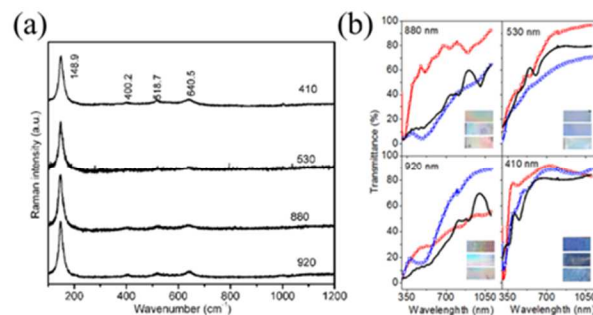


**Figure 5** (a) Raman spectra of 2D-TiO<sub>2</sub> IO films on ITO glass substrates (b) UV-vis-NIR transmittance spectra of PS opal films (black solid line), PS/TiO<sub>2</sub> opal composite films (red, square) and 2D-TiO<sub>2</sub> IO films (blue, triangular) on ITO glass substrate. Inset shows optical reflection images from PS opal (top), PS/TiO<sub>2</sub> opal composite (middle) and 2D-TiO<sub>2</sub> IO films (bottom) on ITO substrates.

UV-vis-NIR transmittance spectra of PS opal, NC anatase PS/TiO<sub>2</sub> opal composite, and NC anatase TiO<sub>2</sub> IO monolayer films on ITO/glass substrates are shown in Figure 5(b). The transmission spectra are presented along with their corresponding optical reflection images (see insets). One can see an obvious color change which depends on the wavelength absorbed by the photonic band gap as the sizes of PS templates change. A single color is distinct for PS410 (blue), PS530 (pale-blue), while PS880 and PS920 appeared as polychrome. For NC anatase PS/TiO<sub>2</sub> opal composite films, the colors spanned from dark blue to polychrome. After the removal of the PS templates, the color of the NC anatase TiO<sub>2</sub> IO monolayer films changed again. Typically, for the sample on ITO glass substrate templated with 410 nm PS spheres, the absorption maxima for the PS opal crystal was measured to be ~450 nm (blue color); while for the NC anatase PS/TiO<sub>2</sub> opal composite it is at 420 nm (blue purple) and at ~520 nm (teal) for NC anatase 2D-TiO<sub>2</sub> IO film. These color changes are attributed to the changes in the effective refractive index for PS opal, PS/TiO<sub>2</sub> opal composite, and NC anatase 2D-TiO<sub>2</sub> IO

films. The effective refractive index for the opal PS film is defined as the following,

$$n_{\text{eff}}(\text{PS opal}) = \sqrt{n_{\text{PS}}^2 F_V + n_{\text{air}}^2 (1 - F_V)}, \quad (1)$$

where  $n_{\text{PS}}$  ( $= 1.59$ ) is the refractive index of PS spheres,  $F_V$  is the volume fraction of PS, and  $n_{\text{air}}$  is the refractive index of air. The volume fraction of PS spheres is obtained from the ratio of the volume of the spheres occupying a hexagonal prism to the volume of the hexagonal prism, and is found to be 0.6046. Applying these values in equation 1, the effective refractive index of the PS opal structure was found to be 1.39. For the  $\text{TiO}_2$ -PS opal composite, anatase  $\text{TiO}_2$  has replaced the air voids, and by replacing the refractive index of air by the refractive index of anatase  $\text{TiO}_2$ , which is 2.30 we get equation 2.<sup>18</sup>

$$n_{\text{eff}}(\text{PSopal}+\text{TiO}_2) = \sqrt{n_{\text{PS}}^2 F_V + n_{\text{TiO}_2}^2 (1 - F_V)} \quad (2)$$

The refractive index of PS- $\text{TiO}_2$  opal composite is thus calculated as 1.90. The removal of the PS spheres resulted in the NC anatase 2D- $\text{TiO}_2$  IO film, whose effective refractive index was calculated using equation 3,

$$n_{\text{eff}}(\text{TiO}_2\text{-IO}) = \sqrt{n_{\text{air}}^2 F_V + n_{\text{TiO}_2}^2 (1 - F_V)}. \quad (3)$$

Considering the volume fraction ( $F_V$ ) of  $\text{TiO}_2$  to air as being the same as that of PS spheres to air in equation 1, the effective refractive index of 2D- $\text{TiO}_2$  IO film was calculated to be 1.64.<sup>20</sup>

#### Discussion on the formation of crack-free 2D- $\text{TiO}_2$ IO films

The formation of large area crack-free 2D- $\text{TiO}_2$  IO films on ITO/glass substrates is attributed to two important processes: the use of an already crystallized  $\text{TiO}_2$  colloidal solution; and an improved 'dynamic-hard-template' infiltration strategy. In this study, a highly dispersive non-aggregated anatase  $\text{TiO}_2$  nanoparticle sol was used. These  $\text{TiO}_2$  nanoparticles enable dense packing and even filling within the interstitial space and consequently the inhomogeneous-shrink-induced cracks has been effectively eliminated. The  $\text{TiO}_2$  nanoparticles were prepared from  $\text{Ti}(\text{i-PrO})_4$  precursor and peptized using TPAOH as crystallisation agent. The final pH of the aqueous solution was  $\sim 10$ . In our work, as a result of the use of preformed crystalline  $\text{TiO}_2$  nanoparticles in the solution, thus avoiding the need for high temperature treatment, the lateral shrinkages of the frameworks were less than 10 % (10 % for the 410 nm PS template; 8.5 % for the 530 nm; 5.3 % for the 880 nm and 1 % for the 920 nm) as compared to greater than 30% with the conventional method.<sup>9, 21</sup> The shrinkage was estimated from the ratio of the diameter of the IO macropores to the diameter ( $\varnothing$ ) of the corresponding template spheres ( $1 - [\varnothing_{\text{IO macropore}}/\varnothing_{\text{template}}] \times 100\%$ ).<sup>21</sup>

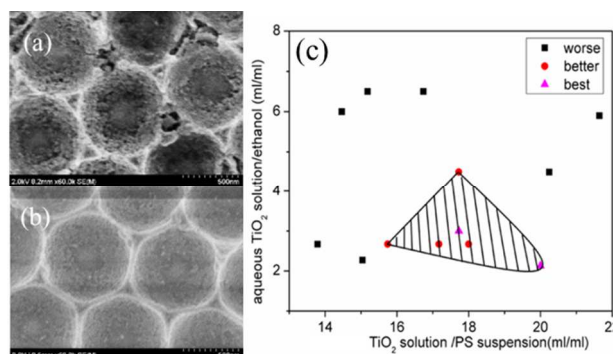


**Figure 6** Comparison for 2D- $\text{TiO}_2$  IO samples templated by 880 nm PS spheres: (a) when an aqueous anatase  $\text{TiO}_2$  solution was directly used, (b) when the aqueous anatase  $\text{TiO}_2$  solution was mixed with ethanol. Relationship between volume ratio of aqueous  $\text{TiO}_2$  solution to ethanol, and volume ratio of  $\text{TiO}_2$  solution to PS suspension for achieving the infiltration and the shadowed part is the optimised ratio-domain for which neck-like framework of the 2D- $\text{TiO}_2$  IOs can be obtained.

It was found that the composition of the sol of preformed crystalline  $\text{TiO}_2$  nanoparticles play an important role in the infiltration process and hence in the control of the thickness of the 2D- $\text{TiO}_2$  IO films. Capillary action is the main force responsible for the filling of the interstitial space between the PS spheres. This capillary action relies on the surface tension of the  $\text{TiO}_2$  sol and the wettability between hydrophobic PS spheres and the sol. When the aqueous sol of preformed crystalline  $\text{TiO}_2$  nanoparticles was directly used, low infiltration filling fraction resulted in low dish-like framework with the existence of some voids, especially among the triangular sites (Fig. 6a). This is due to the presence of TPAOH in the aqueous  $\text{TiO}_2$  sol. Although, TPAOH as surfactant improves the wettability, it lowers the surface tension significantly. In order to improve the infiltration into the PS opals, the aqueous sol of preformed crystalline  $\text{TiO}_2$  nanoparticles was mixed with ethanol. The mediation of ethanol overcomes the deleterious effect of TPAOH and improves the surface tension of the aqueous  $\text{TiO}_2$  sol. The concentration diffusion, the evaporative property of ethanol, as well as the improved wettability of the solution are sufficient to bring the anatase  $\text{TiO}_2$  nanoparticles lifted up to a 'neck-like' height within the interstitial space (Fig. 6b). The proper volume ratio of the aqueous  $\text{TiO}_2$  solution to ethanol was established to be between 2.2 to 4.6 in this study as illustrated in Fig. 6c. In order to demonstrate the efficient infiltration of  $\text{TiO}_2$  nanoparticles, which contributes to the thickness of the IO structure, a cross-sectional SEM image at an angle of  $50^\circ$  (Fig. 7) was obtained for a 2D- $\text{TiO}_2$  IO sample templated from 880 nm PS spheres, prepared using the optimised conditions shown in Fig. 6c. The thickness for the film was measured to be as thin as 668 nm. A ratio of the aqueous  $\text{TiO}_2$  solution to ethanol lower than 2.2 was found to destroy the PS opal monolayer due to excessive low surface tension.

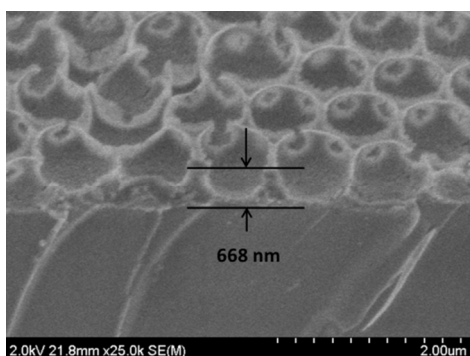


**Figure 7** Cross-sectional SEM image of a 2D-TiO<sub>2</sub> IO film templated by PS spheres of 880 nm diameter, to observe the thickness. (Sample tilted at 50 °)

### Crack-free 2D-TiO<sub>2</sub> IO films coated on ITO/PET substrates

The success of the improved ‘dynamic-hard-template’ infiltration strategy for the fabrication NC-anatase 2D-TiO<sub>2</sub> IO films on ITO glass substrates prompted us to apply it for flexible ITO/PET substrates. First a PS spheres opal crystal on an ITO/PET substrate is fabricated by using the floating route. Figure 8(a) shows a photograph of the isolated opal monolayer on the entire surface of the ITO/PET slide (2.5 cm x 7.5 cm).

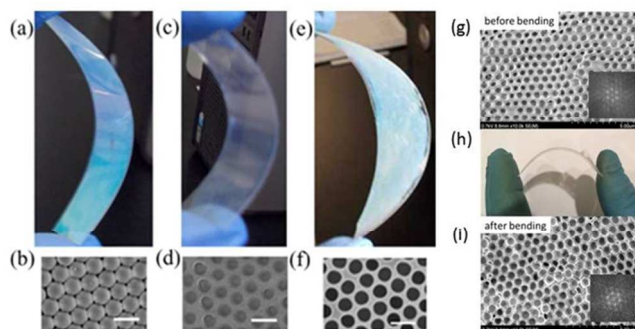


**Figure 8** Photos and SEM images for 2D PS opal ((a) and (b)); PS/TiO<sub>2</sub> opal composite ((c) and (d)) and anatase 2D-TiO<sub>2</sub> IO films ((e) and (f)) on soft ITO/PET substrates templated by PS spheres of diameters 410 nm. Scale bars in the SEM images: 500 nm. (g) SEM image of the 2D-TiO<sub>2</sub> IO (obtained from 880 nm) before bending and the inset showing the forward Fourier transform (FFT) of the SEM image to indicate the periodicity (h) Typical bending of the 2D-TiO<sub>2</sub> IO on flexible substrate (i) SEM image of the same 2D-TiO<sub>2</sub> IO of the sample after bending, with the inset showing the FFT to demonstrate the conservation of periodicity of IO structure after bending.

The opal monolayer shows a blue opalescence under white light illumination, revealing its order and uniform arrangement. The SEM observation (Fig. 8(b)) shows a hexagonally close-packed arrangement of the PS spheres forming a 2D colloidal crystal with long range order. Subsequently, we proceeded to the fabrication of large area crack-free NC anatase 2D-TiO<sub>2</sub> IO films. Figures 8(c) to (f) demonstrate the efficient fabrication of the PS/TiO<sub>2</sub> opal composite followed by the formation of the 2D-TiO<sub>2</sub> IO films after the removal of the PS spheres.<sup>7</sup> Figure 8(c) shows a photograph of the PS/TiO<sub>2</sub> opal composite after the drying step. The sample clearly displayed blue purple opalescence which indicates that the long-range order of the crystal is not disturbed. The SEM image (Fig. 8(d)) shows that

the interstitial space in the colloidal crystal, formed by the highly organized PS monolayer, is well filled by the NC TiO<sub>2</sub> network. The opal template is subsequently removed by THF to create the NC 2D-TiO<sub>2</sub> IO structure. Figure 8(e) shows a picture of the iridescent sample which implies a high degree of order inside the structure. The SEM image (Fig. 8(f)) shows that a high quality NC 2D-TiO<sub>2</sub> IO film is obtained on the ITO/PET substrate. In order to establish the quality of the film before and after bending, SEM images of a typical 2D-TiO<sub>2</sub> IO obtained from 880 nm PS spheres was submitted to a bending cycle. Figure 8(g) shows the SEM image of the sample before bending. Inset shows the Forward Fourier Transform of the same image to indicate the excellent periodicity of the IO structure. Figure 8(h) shows a photograph of the actual bending cycle. Figure 8(i) show the SEM image of the sample after bending and inset shows the periodicity of the IO structure. From Fig. 8(i), it is clear that, the film is able to sustain the bending without any damage to the original structure and the Forward Fourier Transform confirms that the periodicity is sustained after the bending cycle.

Figure 9(a) shows the Raman spectra of the PS opal crystal, PS/TiO<sub>2</sub> opal composite and the 2D-TiO<sub>2</sub> IO monolayer films on ITO/PET substrates. In the spectra of PS/TiO<sub>2</sub> opal composite and 2D-TiO<sub>2</sub> IO monolayer films, the modes emerging at 149.3, 401.7, and 519.5 cm<sup>-1</sup> are the characteristic Raman bands of the TiO<sub>2</sub> in the anatase phase.<sup>18,19</sup> The Raman peaks emerging from the PET substrate and the PS spheres are indicated in the figure. Also, the anatase main band is high-frequency shifted (149.3 cm<sup>-1</sup>) indicating that the TiO<sub>2</sub> is constituted of TiO<sub>2</sub> nanoparticles with particle size of 5.5 nm.<sup>18,19</sup> Figure 9(b) shows the UV-vis-NIR transmittance spectra of the PS opal crystal templated with PS spheres of 410 nm in diameter, NC anatase PS/TiO<sub>2</sub> opal composite and NC anatase 2D-TiO<sub>2</sub> IO monolayer films on ITO/PET substrates. The absorption maxima for the PS opal (456 nm), the PS/TiO<sub>2</sub> opal composite (402 nm) and the NC anatase 2D-TiO<sub>2</sub> IO (519 nm) films are similar for both ITO glass and ITO/PET substrates.

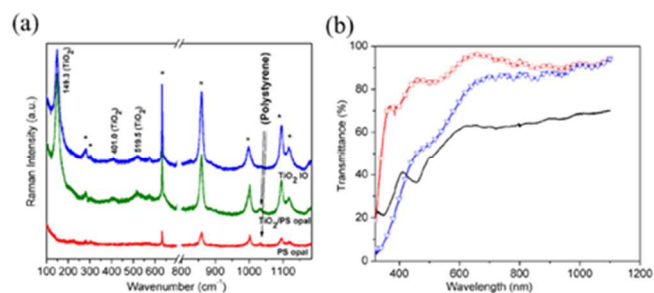


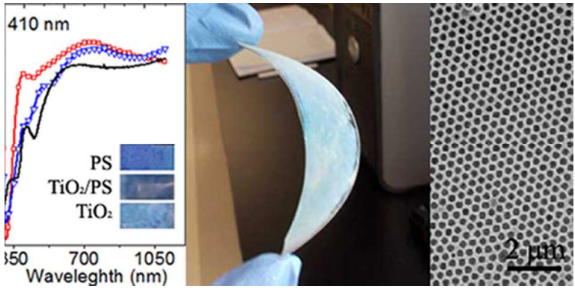
**Figure 9** (a) Raman spectra of PS opal, PS/TiO<sub>2</sub> opal composite and 2D-TiO<sub>2</sub> IO films on soft ITO/PET substrates templated by 410 nm PS spheres. The peaks indicated by \* and arrows are emerging from the ITO/PET substrate, and the PS spheres, respectively. (b) Corresponding UV-vis-NIR transmittance spectra of PS opal (solid line), PS/TiO<sub>2</sub> opal composite (squares) and 2D-TiO<sub>2</sub> IO films (triangles).

### Construction of flexible EC device using 2D-TiO<sub>2</sub> IO films



- 10 E. S. Kwak, W. Lee, N.-G. Park, J. Kim, H. Lee, *Adv. Funct. Mater.*, 2009, **19**, 1093.
- 11 P. Jiang, J. F. Bertone, V. L. Colvin, *Science*, 2001, **291**, 453.
- 12 J. H. Moon, Y. Xu, Y. Dan, S. M. Yang, A. T. Johnson, S. Yang, *Adv. Mater.*, 2007, **19**, 1510.
- 13 Q. Li, J. K. Shang, *J. Am. Ceram. Soc.*, 2008, **91(2)**, 660.
- 14 O. D. Velev, E. W. Kaler, *Adv. Mater.*, 2000, **12**, 531.
- 15 Q. B. Meng, C. H. Fu, Y. Einaga, Z. Z. Gu, A. Fujishima, O. Sato, *Chem. Mater.*, 2002, **14**, 83.
- 16 J. Yu, Q. Yan, D. Shen, *ACS Appl. Mat. Inter.*, 2010, **2**, 1922.
- 17 S. Balaji, Y. Djaoued, A.-S. Albert, R. Brüning, N. Beaudoin, J. Robichaud, *J. Mater. Chem.*, 2011, **21**, 3940.
- 18 Y. Djaoued; S. Badilescu; P. V. Ashrit; D. Bersani; P.P. Lottici, R. Brüning, *J. Sol-Gel Sci. Tech.*, 2002, **24**, 247-254.
- 19 S. Balaji, Y. Djaoued, J. Robichaud, *J. Raman Spectrosc.*, 2006, **37**, 1416.
- 20 K. S. Napolskii, N. A. Sapoletova, D. F. Gorozhankin, A. A. Eliseev, D. Y. Chernyshov, D. V. Byelov, N. A. Grigoryeva, A. A. Mistonov, W. G. Bouwman, K. O. Kvashnina, A. V. Lukashin, A. A. Snigirev, A. V. Vassilieva, S. V. Grigoriev, A. V. Petukhov, *Langmuir*, 2010, **26(4)**, 2346.
- 21 J. E. G. J. Wijnhoven, L. Bechger, and W. L. Vos, *Chem. Mater.*, 2001, **13**, 4486-4499

## Table of contents

<p>Hua Li, Guillaume Vienneau, Martin Jones, Balaji Subramanian, Jacques Robichaud &amp; Yahia Djaoued *</p>	 <p>The figure consists of three parts. On the left is a UV-Vis absorption spectra plot with the x-axis labeled 'Waveleghth (nm)' ranging from 350 to 1050. Three curves are shown: a red curve for PS, a blue curve for TiO<sub>2</sub>/PS, and a black curve for TiO<sub>2</sub>. A peak at 410 nm is marked on the red curve. In the middle is a photograph of a flexible, light-blue film being bent. On the right is an SEM image showing a porous, inverse opal structure with a 2 μm scale bar.</p> <p>A 'Dynamic Hard-Template' Strategy is developed to large-area crack-free synthesis of two-dimensional anatase TiO<sub>2</sub> inverse opal (IO) film on rigid and flexible transparent conducting substrates by using PS templates.</p>
<p>Crack-Free 2D-Inverse Opal Anatase TiO<sub>2</sub> Films on Rigid and Flexible Transparent Conducting Substrates : Low Temperature Large Area Fabrication and Electrochromic Property</p>	